

# Analysis of masonry columns by a 3D F.E.M. homogenisation procedure

A. BARBIERI, A. CECCHI

Dipartimento di Costruzione dell'Architettura

Università IUAV di Venezia

Dorsoduro, 2206 - Venice

ITALY

<http://www.iuav.it>

*Abstract:* - In this work masonry, made of clay bricks and mortar joints, has been investigated. In particular the study of masonry columns - typical of historical buildings and churches - subject to eccentric loads has been carried out taking into account the sensitivity respect to several geometrical and mechanical parameters of the behaviour of this structural element. The difficulty in modelling masonry lies in its heterogeneous character, since it is composed by blocks between which mortar joints are laid. Moreover the block stiffness is very higher than the mortar one. Here a linear elastic analysis is performed that is significant under service loads. For this reason the determination of homogenised elastic properties for in-plane loaded and out-of plane loaded masonry walls has, in recent years, been the object of a number of studies [1, 2, 3]. The masonry has been identified with a standard elastic continuum by means of a homogenisation method. This method allows to determine values of homogenised axial and bending moduli, for different brick pattern, such as to obtain, starting from a 3D heterogeneous model a beam homogeneous 1D model that takes into account the effective micro-structure of masonry column.

The 1D masonry column constants are defined as function of geometrical parameters (size of block and mortar thickness) and as function of mechanical parameters (Young modulus and Poisson ratio of block and mortar). An extensive numerical analysis has been carried out to investigate the capacity of the homogenisation method to grasp the effect of geometrical and mechanical parameters in the analysis of masonry columns with equal cross section and different textures. The sensitivity of displacement field to masonry texture is investigated on a meaningful case such as a masonry column loaded by a horizontal force.

*Key-Words:* - Masonry, Homogenisation technique, Flexural and Axial stiffness, Load bearing capacity

## 1 Introduction

Bearing masonry columns are structural elements present in our historical heritage. This is the reason of the interest in their behaviour, also from a conservation and restoration point of view. These elements generally bear the load induced by floor deck, roof and the upper side of masonry wall; in few cases these bear the own weight. Many researches were carried out following different approaches, especially taking into account the no tensile resistance of masonry. Anyway a linear elastic analysis may be of interest to investigate the masonry behaviour under service loads.

The high number of freedom degrees represents a not negligible drawback. Hence numerical models are computationally very onerous, this is the reason to use continuous models [4, 5, 6, 7].

The development of models is strictly connected to the typology of masonry structure that must be investigated ( columns, panels, arches and domes) and to the definition of the most relevant actions to

which each masonry member may be assumed to be subject. In plane actions [8, 9, 10, 11] - i.e. self-weight, mutual actions between adjacent walls and live loads - may be the most relevant phenomena which brought to a series of studies on masonry. Hence the wide set of 2D models [12, 13, 14, 15].

But also the actions defined as out of plane actions are relevant. These actions are related to the effects of seismic events and also to wind effect and in some case actions due to the connections of the vertical members with horizontal members or to the connections between orthogonal walls. Furthermore - if the actions are out of plane - the model allows to define the bending stiffness [16, 17, 18, 19, 20].

Here a continuous model based on an homogenisation approach is considered. In fact this approach links the masonry behaviour on the micro-level to the macro-level, to take into account global and local phenomena of masonry [21, 22, 23, 24]. The homogenisation approach starts considering mechanical and geometrical properties of single masonry constituents (blocks and mortar joints) and

identify an elementary cell, which regular repetition describe the body as a whole. In this way the field problem is led to the unit cell reducing the computation effort and carrying out average values of mechanical properties.

The masonry is modelled as an heterogeneous material made of blocks and joints which geometrical characteristics vary depending on masonry texture. Different textures are considered as reported in the following paragraph. Moreover also the mechanical characteristics should be different depending on original materials and time of construction, especially referring to historical heritage. For this reason it is useful to evaluate as these aspects could be influent on mechanical parameters as axial and flexural stiffness. Starting from a 3D heterogeneous problem, by means of a homogenisation procedure, the micromechanical 3D kinematic and static descriptors and constitutive prescriptions were transferred to a 1D model. Hence analytical solutions of the macroscopic field problem may be obtained. In this way the last one can take into account the micro-mechanical properties of masonry reducing the computational effort. To evaluate the reliability of the 1D homogenised model a 3D F.E. model has been performed. A numerical analysis has been carried out by comparing the stress along a specific cross section and the maximum displacement at the free end, for different textures and head joint thickness.

**2 Basic assumptions**

Three different masonry textures, which are generally present in historical masonry beam columns are considered. The masonry is made of UNI clay bricks (250x120x55 mm), whereas the mortar joint thickness varies ( $s_h=10$  mm for bed joint and  $s_v=10\div30$  mm for head joint). The following textures are considered:

- a) single block (250x250x55 mm) and bed joint;
- b) two blocks, connected by a head joint and bed joint, with same orientation, called stack bond masonry;
- c) two blocks, connected by a head joint and bed joint, rotated by 90°, called running bond masonry.

Let be  $(x)$  a reference system for the global description of the masonry beam column, called  $\mathfrak{S}$  in the macroscopic scale and let be  $(y)$  a reference system for the elementary module Y-REV. The Y module, as shown in figure 1 may be defined as 0:

$$Y = \left[ -\frac{t_1}{2}, \frac{t_1}{2} \right] \times \left[ -\frac{t_2}{2}, \frac{t_2}{2} \right] \times \left[ -\frac{t_3}{2}, \frac{t_3}{2} \right] = \omega \times \left[ -\frac{t_3}{2}, \frac{t_3}{2} \right] \quad (1)$$

$$\omega = \left[ -\frac{t_1}{2}, \frac{t_1}{2} \right] \times \left[ -\frac{t_2}{2}, \frac{t_2}{2} \right]$$

where  $t_i$  are the 3 dimensions of Y, according to 3 axes directions;  $\omega$  is the cross section of beam column and  $t_3$  is the high of the elementary cell. The boundary of Y is defined as:

$$\partial Y = \partial Y_3^+ \cup \partial Y_3^- \cup \partial Y_\alpha^+ \cup \partial Y_\alpha^- \quad (2)$$

where the Greek index  $\alpha=1,2$ .

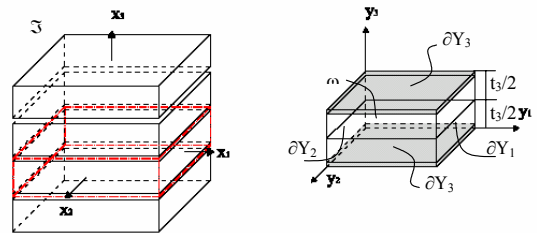


Figure 1 From the elementary cell to Y/8

The Y-REV is described for each masonry texture in figure 2. Due to the symmetry and anti-symmetry plane, as showed in figure 3 on the upper side, the elementary cell may be reduced to 1/8 of it, called Y/8 sub-cell. Each Y/8 is made of brick and mortar following the appropriate texture. The elementary cell of running bond texture exhibits the  $t_3$  dimension bigger than the ones of the others two textures. This aspect is due to the staggered alignment of head joints.

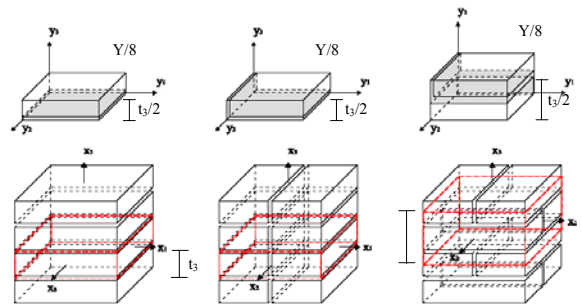


Figure 2 Elementary cell used in analysis and 1/8 of it.

**3 Homogenisation procedure**

Heterogeneous materials may be studied using homogenization techniques that permit the definition of a homogeneous body, equivalent to a strongly heterogeneous one in its geometry and in the properties of its constituent materials. The application of these techniques is tied to the

assumption of the body "periodic" structure; then the body is obtained by the regular repetition of non-homogeneous REV, whose dimensions are small relative to the overall size of the body itself.

Here a simplified model is presented relative to the case of beam column subjected only to normal stresses. The constitutive law of masonry, to model Euler beam column (i.e. shear effects are not taken into account), is expressed in terms of its 3D characteristics. The following auxiliary problem is solved on the elementary cell:

$$\begin{cases} \operatorname{div} \boldsymbol{\sigma} = 0 \\ \boldsymbol{\sigma} = \mathbf{a}(y) \boldsymbol{\varepsilon} \\ \boldsymbol{\varepsilon} = \mathbf{E} + y_\alpha \boldsymbol{\chi} + \operatorname{sym}(\operatorname{grad} \mathbf{u}^{\text{per}}) \\ \boldsymbol{\sigma} e_\alpha = 0 \text{ on } \partial Y_\alpha \\ \boldsymbol{\sigma} e_3 \text{ anti-periodic on } \partial Y_3^\pm \\ \mathbf{u}^{\text{per}} \text{ periodic on } \partial Y_3^\pm \end{cases} \quad (3)$$

where  $\boldsymbol{\sigma}$  is the Cauchy stress tensor;  $\boldsymbol{\varepsilon}$  is the strain tensor;  $\mathbf{E}$  is the macroscopic axial strain tensor;  $\boldsymbol{\chi}$  is the curvature tensor and  $\mathbf{u}^{\text{per}}$  is a periodic displacement field on  $\partial Y_3$ ;  $\mathbf{a}$  is the constitutive function defined as:  $\mathbf{a}^{\text{B}}$  for  $y \in \text{block}$  and  $\mathbf{a}^{\text{M}}$  for  $y \in \text{mortar}$  with  $\mathbf{a}^{\text{B}}$  and  $\mathbf{a}^{\text{M}}$  are respectively the block and the mortar constitutive law. Both the materials are assumed isotropic. The field equation (3) will be used for the numerical solution of the problem.

The macroscopic tensors are related to the macroscopic displacement field ( $U_1(x_3)$ ,  $U_2(x_3)$  and  $U_3(x_3)$ ) components as follows:

$$E_{ij} = \frac{1}{2}(U_{i,j} + U_{j,i}) \quad (4)$$

where the Latin index  $i, j=1,2,3$ . In particular, due to the hypothesis of normal stress, the only  $E_3$  component is considered different to zero. The relationship between the displacement field and the curvature tensor is:

$$\chi_\alpha = \varphi_{\alpha,3} = -U_{\beta,33} \quad (5)$$

where  $\varphi_\alpha$  is the rotation of beam cross section. The index  $\alpha$  identify the rotation axis.

Due to the 1D nature of the problem, the homogenised constitutive law of the beam subjected to eccentric axial loads, in the case of central symmetry, becomes:

$$\begin{aligned} N_3 &= \langle \sigma_3 \rangle = H_{33} E_3 \\ M_\alpha &= \langle y_\beta \sigma_3 \rangle = D_{\alpha\alpha} \chi_\alpha \end{aligned} \quad (6)$$

where  $\langle \cdot \rangle$  is the average operator defined as:

$$\langle f \rangle = \frac{1}{t_3} \int_Y f(y_1, y_2, y_3) dy_1 dy_2 dy_3 \quad (7)$$

#### 4 F.E.M. Homogenisation procedure

A numerical method was applied to evaluate the axial  $H_{33}$  and flexural  $D_{\alpha\alpha}$  homogenised moduli for a 3D beam column analysing different masonry textures as reported in paragraph 2. The field problem of the elementary cell may be reported to the Y/8 due to the symmetry planes. The periodic boundary conditions that must be imposed are:

$$u_3(\mathbf{y}) = E_3 y_3 + (\chi_1 y_2 - \chi_2 y_1) y_3 + u_3^{\text{per}}(\mathbf{y}) \quad (8)$$

in particular three relevant cases are considered:

$$\chi^{(1)} = (1); \quad \chi^{(2)} = (1); \quad E^{(3)} = (1); \quad (9)$$

hence:

- axial elongation along  $y_3$  axis:

$$u_3(\mathbf{y}) = E^{(3)} y_3 + u_3^{\text{per}}(\mathbf{y})$$

- curvature around  $y_1$  axis:

$$u_3(\mathbf{y}) = y_2 \chi^{(1)} y_3 + u_3^{\text{per}}(\mathbf{y})$$

- curvature around  $y_2$  axis:

$$u_3(\mathbf{y}) = -y_1 \chi^{(2)} y_3 + u_3^{\text{per}}(\mathbf{y})$$

The imposed suitable boundary conditions for  $u^{\text{per}}$  periodic on  $\partial Y_3^\pm$  are plotted in figure 3.

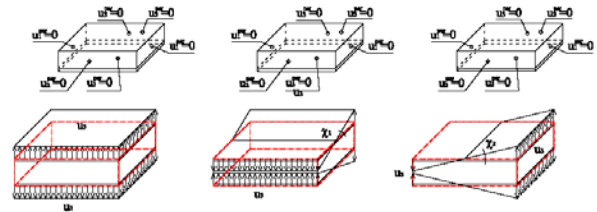


Figure 3 Displacement conditions on elementary cell

The Y/8 module is defined as follows:

$$Y/8 = \left[ 0, \frac{t_1}{2} \left[ \times \right] 0, \frac{t_2}{2} \left[ \times \right] 0, \frac{t_3}{2} \left[ \right. \right] \quad (10)$$

The homogenised axial and flexural moduli are evaluated by numerical model on the Y/8 solving field problem (3). Hence it is:

$$\begin{aligned} H_{33} &= \frac{8}{t_3} \int \sigma_3 dV \\ D_{\alpha\alpha} &= \frac{8}{t_3} \int \sigma_3 y_\beta dV \end{aligned} \quad (11)$$

where  $t_3$  is the thickness of elementary cell.

The F.E. model is based on the following assumption as showed in 0:

1. perfect continuity between joint and block;
2. the periodic displacement fulfils the constant/linear assumption, at the boundary of the cell, of the macroscopic kinematics descriptors  $\mathbf{E}$  and  $\boldsymbol{\chi}$ .

The finite element model has been built for each masonry texture, meshing the  $Y/8$ . Three elements are used in the discretisation of the mortar joint across its thickness. Both joint and block elements are modelled by 8 nodes elements. The constitutive laws for mortar and brick are linear elastic and isotropic. The mechanical properties of masonry in F.E. model are reported in table 1.

Young modulus [N/mm <sup>2</sup> ]	Poisson ratio
$E^b = 10000$	$\nu^b = 0.2$
$E^m = 1 \div 10000$	$\nu^m = 0.2$

Table 1: Mechanical properties of masonry.

The symmetry of the elementary cell entails a simplification of F.E. model. If the curvature tensor  $\chi_\alpha$  acts, the plane  $y_\beta=0$  is plane of symmetry, whereas the planes  $y_\alpha=0$  and  $y_3=0$  are planes of anti-symmetry. The boundary conditions that must be imposed in the F.E. model for each masonry texture to evaluate the axial modulus  $H_{33}$  and the flexural moduli  $D_{\alpha\alpha}$  are reported in table 2 according to eq. (9):

	$y_1 = 0$	$y_2 = 0$	$y_3 = 0$	$y_3 = t/2$
$H_{33}$	$u_2 = 0$	$u_1 = 0$	$u_3 = 0$	$u_3 = E^{(3)} \cdot t/2$
$D_{11}$	$u_1 = 0$	$u_1 = 0;$ $u_3 = 0$	$u_3 = 0$	$u_3 = y_2 \cdot \chi^{(1)} \cdot t_3/2$
$D_{22}$	$u_2 = 0;$ $u_3 = 0$	$u_2 = 0$	$u_3 = 0$	$u_3 = -y_1 \cdot \chi^{(2)} \cdot t_3/2$

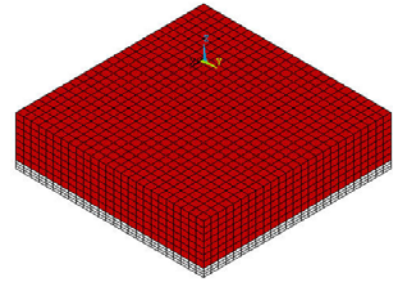
Table 2: Applied boundary conditions at F.E. model.

### 5 Numerical results

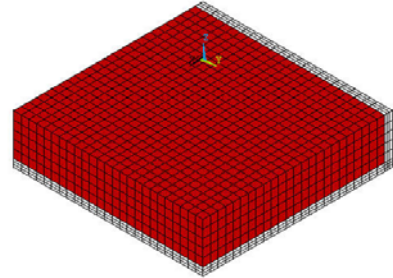
In the following subparagraphs, a numerical experimentation on  $H_{33}$  axial and  $D_{\alpha\alpha}$  flexural homogenised moduli are reported for each masonry texture.  $H_{33} = E^H A^H_{33}$  where  $E^H$  is the Young homogenised modulus of the masonry - block ( $E^b$ ) and mortar ( $E^m$ ) - by assuming block and mortar as isotropic materials;  $A^H_{33}$  is the homogenised cross sections.  $D_{\alpha\alpha} = E^H I^H_{\alpha\alpha}$  where  $I^H_{\alpha\alpha}$  is the homogenised inertia modulus.

In the following figure 4, the mesh of  $Y/8$  for the texture A, B, C is reported.

Texture A



Texture B



Texture C

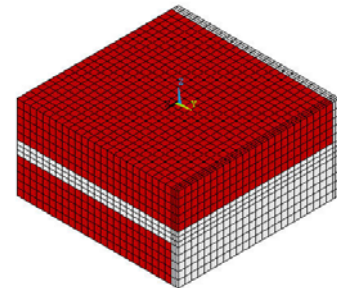


Figure 4  $Y/8$  elementary cell meshing, for texture A, B (stack bond) and C (running bond).

#### 5.1 Analysis of textures

Texture A is the simplest that should be present in the historical heritage. The elasticity has been considered concentrated in the mortar joints. In the numerical and analytical models the block is assumed also elastic (see table 1), in the aim to perform a comparison with the other masonry textures where the hypothesis of rigid blocks may be too restrictive. Obviously, according to the symmetry of cross section, the flexural modulus is the same respect the  $y_1$  and  $y_2$  axis. As expected the proposed F.E. model well fit the 1D analytical one.

Texture B, called stack bond masonry, the thickness of head joint was assumed of 10, 20 and 30 mm respectively to evaluate the influence of the head joint size on axial and flexural moduli. Flexural moduli show differences due to the head joint thickness; this model is more sensitive to head joint size when the curvature acts along the  $y_1$  axis.

The error obtained using the analytical model A, respect to del F.E. model B assuming the same geometrical cross section, increase reducing the ratio between mortar and block Young modulus. Furthermore the maximum value of the error is smaller than 10%.

Also in texture C, called running bond masonry, the thickness of head joint was assumed of 10, 20 and 30 mm. Flexural moduli  $D_{11}$  and  $D_{22}$  do not differ because the head joint is present along both  $y_1$  and  $y_2$  axis. The head joint thickness has influence on axial and flexural moduli, but it is more evident on flexural modulus than on axial one: the increment of flexural stiffness when head joint thickness increases is less or equal to 35%, whereas the increment of axial stiffness is less or equal to 16%, when  $E^m/E^b=1$ . The increment of head joint thickness size induces an increment in beam column stiffness due mainly to the increment of cross section. In fact this sensitivity is not present on axial stiffness variation.

The error obtained using the analytical model A, respect to the F.E. model C, increase when the ratio between mortar and block Young modulus tends to zero; and it is smaller than 10%. The error obtained is more consistent when the analytical model A is applied to evaluate the axial stiffness with the ratio  $E_m/E_b=10^{-4}$ , as for the previous masonry texture. The numerical results are reported detailed in [27].

### 5.2 Comparison between masonry textures

Comparing stack bond and running bond masonry textures, the sensitivity to the bond and to the head joint thickness dimension is evaluated.

The diagrams of figure 5 and 6 show the flexural modulus  $D_{11}$  and  $D_{22}$  versus  $E^m/E^b=0.2\div 0.4$  respectively.

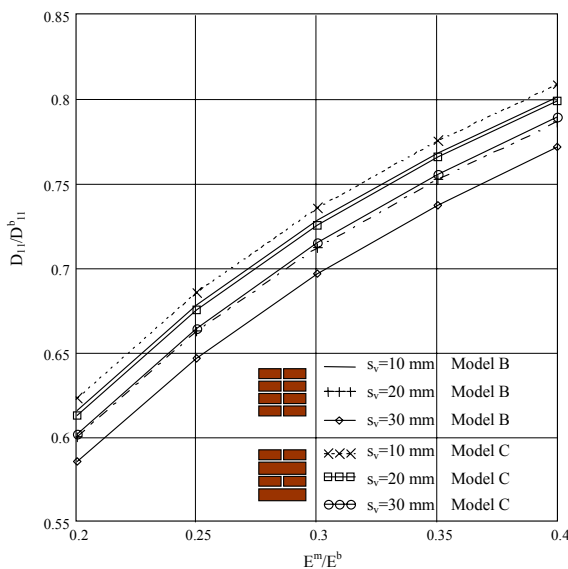


Figure 5  $D_{11}$  comparison between masonry texture B and C respect to homogeneous model between  $E^m/E^b=0.2\div 0.4$ .

Referring to  $D_{11}$  The stack bond masonry texture (type B) is more deformable than the running bond masonry texture because the head joint is not continuous along the  $y_3$  axis and it is continuous along  $y_2$  axis. Increasing the head joint thickness, that is composed by mortar – the more deformable material –, the deformability decreases. This phenomena is more evident in texture type B. Referring to  $D_{22}$ , the texture B is not sensitive on head joint thickness increment, where as the texture C shows the same results along  $y_1$  and  $y_2$  axis. More attention has to be done analysing masonry elements with stack bond texture, especially if the load acts along the head joint plane.

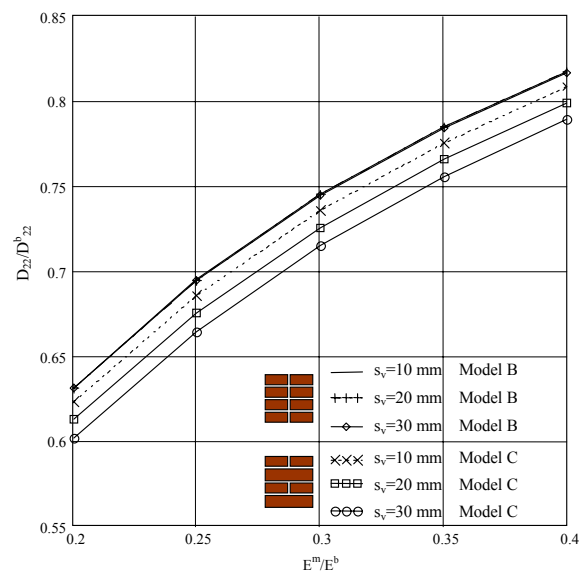
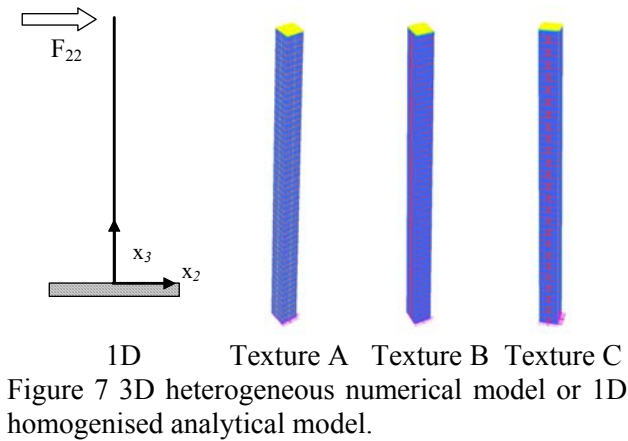


Figure 6  $D_{22}$  comparison between masonry texture B and C respect to homogeneous model between  $E^m/E^b=0.2\div 0.4$ .

## 6 Masonry column

A 3D full F.E. model as been built to represent masonry column with single block, running bond and stack bond textures. The aim is to compare the 3D heterogeneous model with the homogenised 1D model. Brick elements (8 node) are used both for blocks and for mortar joints (Fig. 7).

The masonry column has a square cross section and it is 3240 mm high. The cross section dimensions depend on head joint thickness, nevertheless the influence of it is more evident for  $s_v=30$  mm. This value was assumed to compare 1D to 3D model.



The column is loaded by an unit horizontal force in both direction ( $F_{11}=1N$  and  $F_{22}=1N$ ) applied at the upper end, whereas the lower end is clamped. The comparison between the 3D full F.E. model and 1D homogenised model is carried out for  $0.1 \leq E^m/E^b \leq 1$ . The displacement  $\delta$  at the free end of a cantilever beam subjected to a transversal force is:

$$\delta = \frac{Fl^3}{3D_{\alpha\alpha}} \quad (14)$$

where  $l$  is the column height.

The displacement of the cross section centre at upper end of 3D model is considered and compared with the same point displacement obtained in 1D model. In figure 8, 9, 10 the ratio between the maximum displacement of 3D numerical model and 1D analytical model respect to 1D model considering homogeneous material ( $E^m=E^b=10$  GPa) is plotted.

The numerical results carried out show that a good agreement between 3D heterogeneous model and 1D homogenised model for each texture. The simulation for texture A and C was carried out only for  $F_{11}$  because of the symmetry in masonry texture along  $y_1$  and  $y_2$  axes, as it was shown in the previous research [27]. The analysis for texture B was done both for  $F_{11}$  and  $F_{22}$  because the flexural behaviour, in this case, is dependent on stack bond joint. The displacement field is different along  $y_1$  and  $y_2$  axes and the discrepancy increases when  $E^m/E^b$  ratio decreases (Fig. 9).

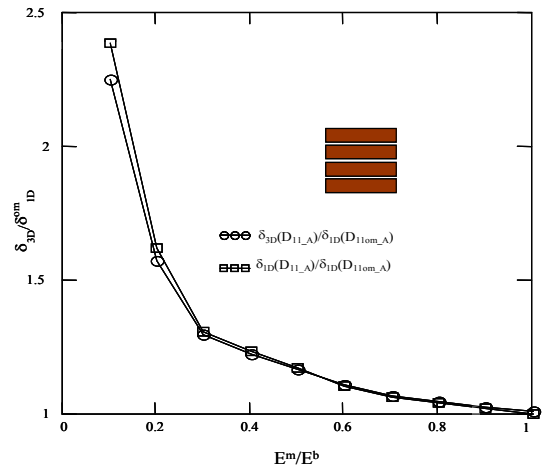


Figure 8 Maximum displacement at top of masonry column for texture A. Comparison between 1D homogenised and 3D heterogeneous models versus  $E^m/E^b$  ratio.

In figures 11, 12, 13 the stress field of the first layers of blocks and head joint is reported. On left side of figures the masonry is heterogeneous ( $E^m=1$  GPa;  $E^b=10$  GPa); while on the right side of figures the masonry is considered as homogeneous ( $E^m=E^b=10$  GPa). It is evident as the stress is uniform along blocks and joint in the homogenous case, where as a gap is recorded between blocks and joints due to heterogeneity of masonry.

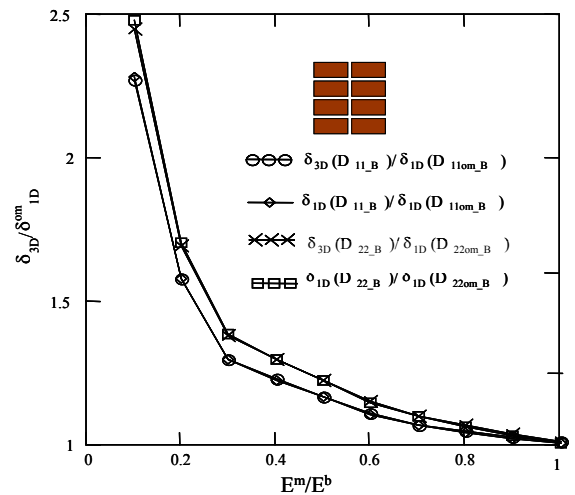


Figure 9 Maximum displacement at top of masonry column for texture B. Comparison between 1D homogenised and 3D heterogeneous models versus  $E^m/E^b$  ratio, for  $F_{11}$  and  $F_{22}$ .

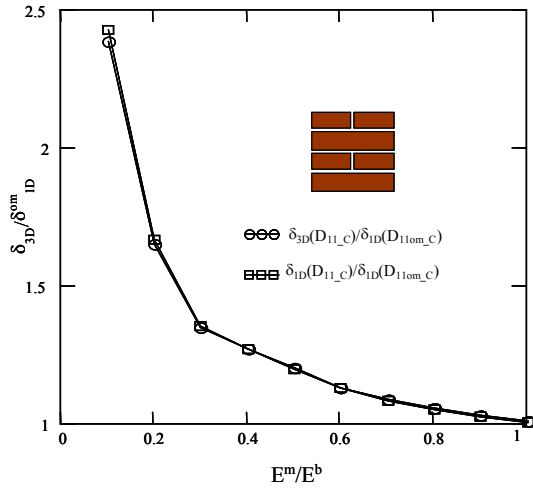


Figure 10 Maximum displacement at top of masonry column for texture C. Comparison between 1D homogenised and 3D heterogeneous models versus  $E^m/E^b$  ratio.

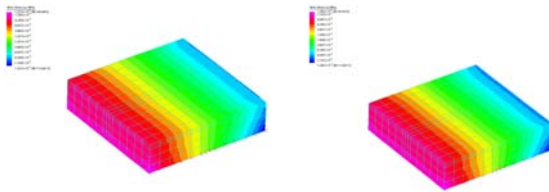


Figure 11 Texture A: stress field of 3D numerical model for heterogeneous and homogeneous material.

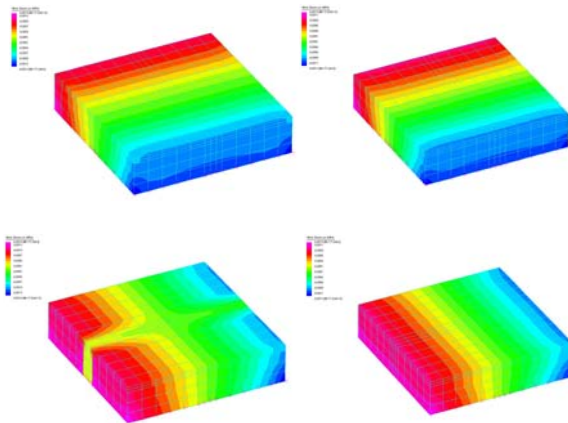


Figure 12 Texture B: stress field of 3D numerical model for heterogeneous and homogeneous material, along  $y_1$  and  $y_2$ .

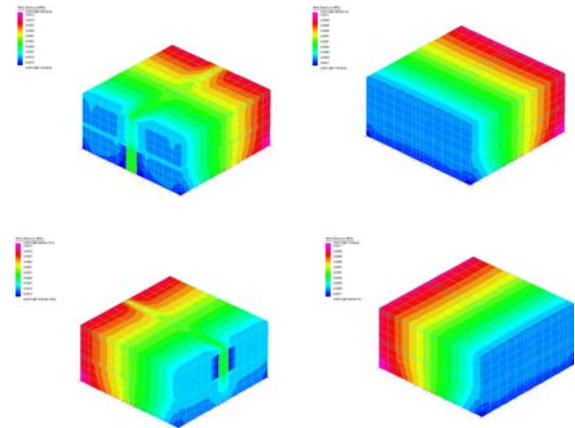


Figure 13 Texture C: stress field of 3D numerical model for heterogeneous and homogeneous material, along  $y_1$  and  $y_2$ .

### 7 Conclusion

The proposed 1D homogenised model allows to investigate easily the axial and flexural behaviour of masonry column, when a wider set of internal parameters varies (i.e. relative size of the joints, relative deformability of the joints).

The 1D homogenised axial and flexural moduli take into account the micro-level (masonry texture) as shown in subparagraph 5.2.

The obtained results, carried out for a meaningful case, show the reliability of the homogenisation procedure. The 1D model here presented is a first step in the study of masonry column behaviour. In particular the idea is to extend this model to a full 1D beam model, in which not only the shear actions are taken into account but also the torque is considered.

### Acknowledgments

The research project reported in this paper was conducted with the financial support of CNR-MIUR, SP3, law 449/97.

### References:

- [1] A. Anthoine, Derivation of in plane elastic characteristics of masonry through homogenisation theory. *International Journal of Solids and Structures*, 32, pp. 137-163, 1995.
- [2] A. Cecchi and K. Sab, A multi-parameter homogenisation study for modelling elastic masonry. *European Journal of Mechanics A/Solids*, 21, pp. 249-268, 2002.
- [3] A. Cecchi and K. Sab, Out of plane model for heterogeneous periodic materials: the case of

- masonry. *European Journal of Mechanics A/Solids*, 21, pp. 715-746, 2002.
- [4] G. Alpa and I. Monetto, Microstructural Model for Dry Block Masonry Walls with In-Plane Loading. *Journal of The Mechanics and Physics of Solids*, 47 (7), pp. 1159-1175, 1994.
- [5] H.R. Lofti, P. Benson Shing, Interface model applied to fracture of masonry structures. *Journal of Structural Engineering*, 120, pp. 63-80, 1994.
- [6] R. Luciano and E. Sacco, Homogenization Technique and Damage Model for Old Masonry Material. *International Journal of Solids and Structures*, 34 (24), pp. 3191-3208, 1997.
- [7] R. Masiani, N.L. Rizzi and P. Trovalusci, Masonry walls as structured continua. *Meccanica*, 30, pp. 673-683, 1995.
- [8] S. Pietruszczak, X. Niu, A mathematical description of macroscopic behaviour of brick masonry. *International Journal of Solids and Structures*, 29 (5), pp. 531-546, 1992.
- [9] N.G. Shrive and G.L. England, Elastic creep and shrinkage behaviour of masonry. *International Journal of Solids and Structures*, 29, pp. 103-109, 1991.
- [10] S. J. Lee, G.N. Pande and B. Kralj, A Comparative Study on the Approximate Analysis of Masonry Structures. *Materials and Structures*, 61 (4), pp. 735-745, 1998.
- [11] G. De Felice, Metodi di omogeneizzazione per sistemi regolari di corpi rigidi. *Proc. Aimeta*, Napoli, Italy, 1995.
- [12] G. Maier, A. Nappi and E. Papa, On damage and failure of brick masonry. *Experimental and numerical methods in earthquake engineering*, ed. by Donea and P.M. Jones, Ispra, pp. 223-245, 1991.
- [13] G. De Felice, Détermination des coefficients d'élasticité de la maçonnerie par une méthode d'homogénéisation. *Actes du 12ème Congrès Français de Mécanique*, 1, Strasbourg, pp. 393-396, 1995.
- [14] G. Salerno, G. De Felice, Continuum modelling of discrete systems: a variational approach. *Proc. ECCOMAS*, Barcelona, Spain, 2000.
- [15] G.N. Pande, J.X. Liang and J. Middleton, Equivalent elastic moduli for brick masonry. *Comp. Geotechn.*, 8, pp. 243-265, 1989
- [16] P.B. Lourenço, Anisotropic softening model for masonry plates and shells. *Journal o Structural Engineering*, 126 (9), pp. 1008-1015, 2000.
- [17] A. Zucchini and P.B. Lourenço, A micro-mechanical model for homogenisation of masonry. *International Journal of Solids and Structures*, 39, pp. 3233-3255, 2002
- [18] A. Anthoine and P. Pegon, Numerical strategies for solving continuum damage problems involving softening: application to the homogenization of masonry. *Proc. 2<sup>nd</sup> International Conference on Computational Structures Technology*, Atene, 1994.
- [19] S. Chiostrini and A. Vignoli, Application of a numerical method to the study of masonry panels with various geometry under seismic loads. *Structural Repair and Maintenance of historical buildings*, ed. Brebbia, 1989.
- [20] J.M. Gilstrap and C.W. Dolan, Out of plane bending of FRP-reinforced masonry walls. *Composites sciences and Technology*, 58, pp. 1277-1284, 1998.
- [21] J. Lopez, S. Oller, E. Onate and J. Lubliner, A homogeneous constitutive model for masonry. *International Journal Numerical Methods in Engineering*. 46 (10), pp. 1651-1671, 1999.
- [22] A. Cecchi, G. Milani and A. Tralli, Validation of analytical multiparameter homogenisation model for out-of-plane loaded masonry walls by means of the finite element method. *Jour. of Engineering Mechanics*, 131(2), pp. 185-198, 2005.
- [23] S.J. Lee, G.N. Pande, J.Middleton and B. Kralj, Numerical modelling of brick masonry panels subject to lateral loading. *Computers and Structures*, 31 (211), pp. 473-479, 1996.
- [24] X. Zhang, S. Singh, D.K. Bull and N. Cooke, Out of plane performance of reinforced masonry walls with openings. *Journal of Structural Engineering*, 127 (1), pp. 51-57, 2001.
- [25] A. Cecchi, G. Milani and A. Tralli, In-plane loaded CFRP reinforced masonry walls: mechanical characteristics by homogenisation procedures. *Composites Science and Technology*, 64, pp. 2097-2112, 2004.
- [26] A. Cecchi, N.L. Rizzi, Heterogeneous material: a mixed homogeneization rigidification technique. *International Journal of Solids Structures*, 38 (1), pp. 29-36, 2001.
- [27] A Barbieri., A. Cecchi, A. Di Tommaso, 3D homogenisation procedure for load bearing masonry columns. *Proc. ECCOMAS*, Lisbon, Portugal, 2006.